

# PHYS 218C 2021 Spring Lecture notes (Week 2)

Lecturer: Patrick Diamond

Summary: Haotian Mao

University of California, San Diego

(Dated: June 13, 2021)

## CONTENTS

1. Transport in pipe flow	2
2. Mixing Length Theory	6
3. Tokamak Transport	7
A. Dimensionless number	7
B. Dynamic range of DWT	10
C. Theoretical view of the diffusion	13
D. Effect of shear flow	15

### 1. TRANSPORT IN PIPE FLOW

In this section, we take a first view of turbulent transport problem by examine the easiest case, which is pipe flow. The pipe is considered as an inhomogeneous bounded system, where we have the pressure drop  $\Delta p$  along the pipe flow. The flow is driven by the pressure drop per unit length  $\Delta p/l$ . A schematic of the pipe flow problem is shown in FIG. 1. Here, we take the direction of the flow as  $x$ -axis, and the plane of the wall as  $xz$  plane. The flow has a no-slip boundary condition at the wall ( $u_x(y=0) = 0$ ). There is no  $y$  and  $z$  component of the velocity ( $u_y = u_z = 0$ ) and all quantities depend on  $y$  only. To study the turbulence, we are considering case for Reynolds number  $R_e = 2Ua/\nu \gg 1$ , where  $a$  is the radius of the pipe and  $U$  is the mean velocity of the flow. The flow in the pipe is governed by the Navies-Stokes equation:

$$\frac{\partial \mathbf{v}}{\partial t} + \mathbf{v} \cdot \nabla \mathbf{v} = -\frac{\nabla p}{\rho} + \nu \nabla^2 \mathbf{v}. \quad (1.1)$$

Although  $R_e \gg 1$ , we need to keep the resistance term to satisfy the boundary condition.

Because of the no-slip boundary condition, the flow in the pipe experience a drag force due to the friction to the wall. Here, we denote the frictional force on unit area of the surface by  $\sigma$ . It is the momentum transmitted by turbulent mixing per unit time. The  $x$ -component momentum is continuously transmitted from the layers of fluid remote from the surface yo those nearer it, which confines the overall momentum. The existence of the momentum flux

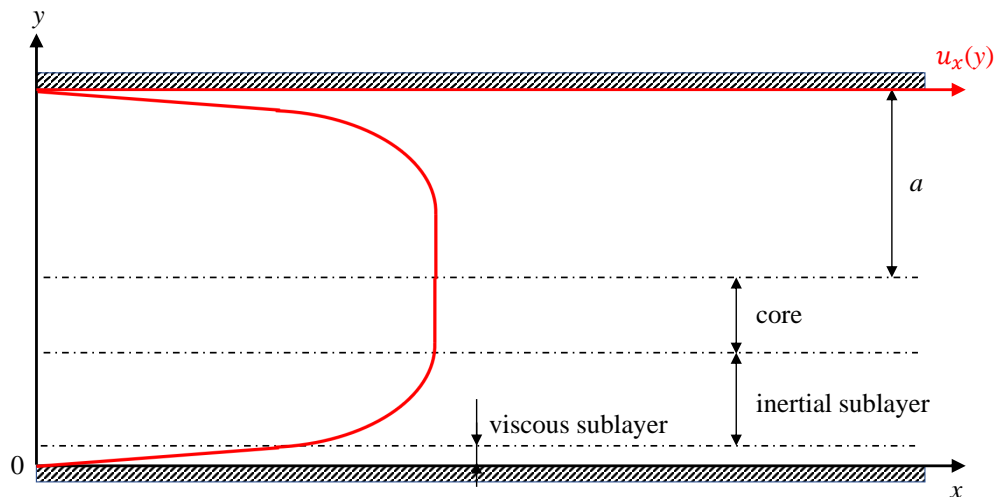


FIG. 1. A schematic of the steady-state velocity profile of pipe flow with a no-slip boundary condition. The red curve denotes the  $x$ -component velocity distribution with  $y$ .

is due to the gradient of the velocity in  $y$ -direction. If there is no boundary condition and we have a homogenized velocity profile, there would be no momentum flux.

At a sufficiently small distance from the surface, the viscosity of the fluid is actually a key factor. We call this layer the viscous sublayer. The thickness of the viscous sublayer is denoted as  $l_{vs}$ . The scale of the turbulence at these distances is of the order of  $l_{vs}$ .

The characteristic velocity of the turbulent  $u_*$  is defined by  $\sigma = \rho u_*^2$ . The term  $u_*$  is called the typical turbulent velocity or the friction velocity. In a steady state, we notice the two key players, namely the friction to the wall and the pressure drop which drives the flow, must be balancing each other. From that we derive the friction velocity  $u_*$

$$2\pi a l \rho u_*^2 = \pi a^2 \Delta p, \quad (1.2)$$

$$u_* = (\Delta p / 2\rho)^{\frac{1}{2}} (a/l)^{\frac{1}{2}}. \quad (1.3)$$

We can estimate the thickness of viscous sublayer by the Reynolds number  $Re \sim u_* l_{vs} / \nu$ . The viscosity would be important when  $Re$  becomes the order of unity. Therefore, we find

$$l_{vs} \sim \nu / u_*. \quad (1.4)$$

At the layer within the viscous sublayer ( $y < l_{vs}$ ), the flow is determined by ordinary

friction. The velocity distribution can be obtained directly by the formula of viscous friction

$$\sigma = \rho u_*^2 = \rho \nu \frac{\partial u}{\partial y}, \quad (1.5)$$

$$u(y) = \frac{u_*^2 y}{\nu} \quad (y < l_{vs}). \quad (1.6)$$

This means the velocity profile in the viscous sublayer is linear with  $y$ .

With a distance further than  $l_{vs}$  to the wall, viscosity become less important. We call this region ( $l_{vs} < y < a$ ) the inertial sublayer. Here it is important to point out the universality of the inertial sublayer, which means the velocity profile in this layer is invariant of the scales we choose. To determine the velocity gradient  $du/dy$ , the only parameters we have left is  $\rho$ ,  $U_*$ , and of course the distance to the wall  $y$ . The only combination with the right dimensions is  $u_*/y$ . Hence we must have

$$du/dy = u_*/y. \quad (1.7)$$

Integration of Eq. (1.7) gives

$$u = u_* \log y + c, \quad (1.8)$$

where  $c$  is a constant of integration. This constant can be determined as there is no sharp boundary between the viscous sublayer and the inertial sublayer. To match the velocity at the viscous layer at  $y = l_{vs}$ , we have  $c = u_*(1 - \log(\nu/u_*))$ . So the velocity profile has

$$u = u_* \log(yu_*/\nu) + u_*. \quad (1.9)$$

This shows that the inertial sublayer has a logarithmic velocity profile.

At the distance near the center of the pipe, the function  $\log y$  varies slowly and we have a near-flat velocity profile in this region (we refer to this region as the core of the flow). With the logarithm accuracy ( $\log(au_*/\nu) \gg 1$ ), we can use the formula Eq. (1.9) to evaluate the mean velocity  $U$  by replacing  $y$  by  $a$

$$U = u_* \log(au_*/\nu). \quad (1.10)$$

We substitute Eq. (1.3) in to Eq. (1.10) which gives,

$$U = \sqrt{(a\Delta p/2\rho l)} \log[(a/\nu)\sqrt{(a\Delta p/2\rho l)}]. \quad (1.11)$$

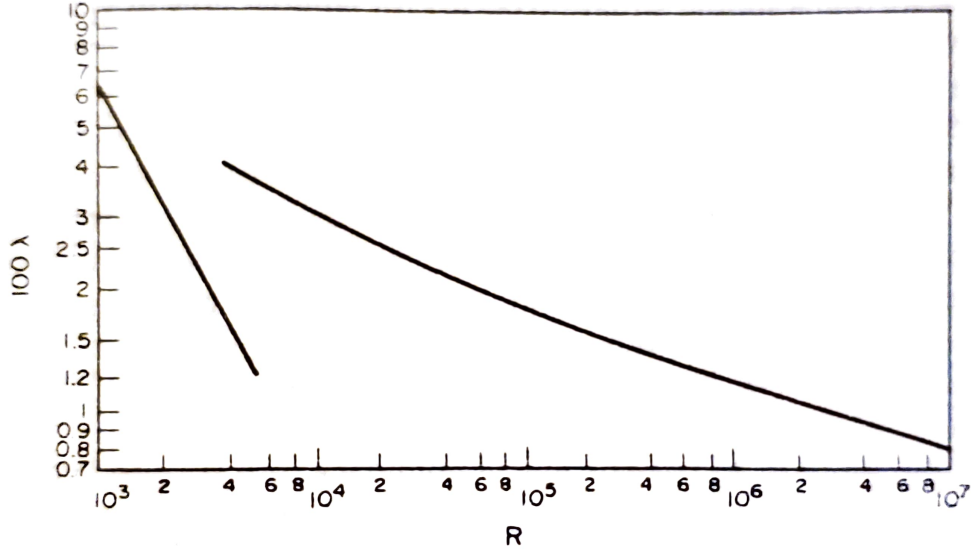


FIG. 2. A logarithmic graph of  $\lambda$  as a function of Reynolds number  $R$ . The first branch (smaller  $R$ ) denotes the laminar flow and the second branch (larger  $R$ ) denotes the turbulent flow.

It is customary to introduce a dimensionless parameter  $\lambda$  called the resistance coefficient of the pipe,

$$\lambda = \frac{2a\Delta p/l}{\frac{1}{2}\rho U^2} \quad (1.12)$$

This parameters shows the ratio of the driving energy (input energy) versus the energy stored in the flow. We can find out the dependence of  $\lambda$  on the dimensionless Reynolds number  $R_e = 2aU/\nu$  in the turbulent using Eq. 1.11 With all the constants considered, the relation gives

$$1/\sqrt{\lambda} = 0.88 \log(R_e \sqrt{\lambda}) - 0.85 \quad (1.13)$$

For comparison, for the laminar flow

$$\lambda = 64/R_e \quad (1.14)$$

. Figure 2 shows a logarithmic graph of  $\lambda$  as a function of  $R_e$ . We observed that the resistance coefficient diminish with the increasing Reynolds number more rapidly than in turbulent flow. At the transit point the resistance coefficient increases abruptly and transit to the less steep turbulent curve.

## 2. MIXING LENGTH THEORY

In the previous section, we studied how the momentum in the pipe flow is confined by the momentum transmission to the wall. The mechanism here is that the momentum is transported to the wall by turbulent mixing, which akin to kinetic theory in gas. It is also important to point out that this procedure is a flux driven transport. We get the momentum flux by calculating Reynolds stress.

The Reynolds stress  $\sigma$  is the mean value of the component  $\Pi_{x,y}$  of the momentum flux density tensor. Outside the viscous sublayer, the viscosity is omitted and  $\Pi_{x,y} = \rho v_x v_y$ . The mean velocity is in x-direction so  $v_x = u + \tilde{v}_x$ ,  $v_y = \tilde{v}_y$ . Previously, we define  $\sigma = \rho u_*^2$  by the assumption that the fluctuation of the turbulent is isotropic ( $\langle v_y v_x \rangle \sim u_*^2$ ). Therefore,

$$\sigma = \rho u_*^2 = \rho \langle v_x v_y \rangle = \rho \langle \tilde{v}_x \tilde{v}_y \rangle. \quad (2.1)$$

To calculate the Reynolds stress, we need to find out the fluctuation of stream-wise velocity  $\tilde{v}_x$ .

Now, we assume that the fluctuation is caused by the transport via distribution of the ‘parcels’ of fluid. The momentum of the parcels are considered to be conserved locally, which means the parcel keeps the momentum from its original location. The fluctuation occurs when the parcel is transported over a distance  $l$ . Then, we can express the fluctuation with Taylor expansion

$$\tilde{v}_x = u(y-l) - u(y) \simeq -l \frac{\partial u}{\partial y}. \quad (2.2)$$

With  $\tilde{v}_y \sim u_*$ , we can express the Reynolds stress as

$$\sigma = -\rho \langle u_* l \rangle \frac{\partial u}{\partial y} \quad (2.3)$$

The term  $\langle u_* l \rangle$  acts like a viscosity term, which can refer it as eddy viscosity or turbulent viscosity. The term  $l$  is called mixing length. It is the length scale over which the mixing of parcel momentum occur. It is important to distinguish it to the mean free path as the discussion above does not involve collisions. The way we described above to study the flux driven transport is called the Mixing length theory (MLT).

It is important to point out the scale invariance in this problem. We don’t have a characteristic constant parameter which might give the fundamental scale of the turbulence. The scale is determined by the distance  $y$  itself. Therefore, the mixing length is restricted

only by the distance to the nearest boundary. Then, with  $l \sim y$ , we substitute it into Eq.2.3

$$\rho u_* y \frac{\partial u}{\partial y} = \rho u_*^2 = \sigma \quad (2.4)$$

which gives the same differential equation as 1.7 and we get the logarithmic profile in inertial layer. The logarithmic profile is also called the ‘Law of the wall’ in turbulent.

With the Taylor expansion in Eq. 2.2, a potential limitation in MLT is that we need the transport to be local. In other words, the mixing length  $l$  has to be small compared to the distance over which mean quantities, like  $u$  here, vary appreciably. However, there is some variation of MLT where we can study a non-local transport. For example, the paper by Spiegel in 1962 solves the calculation of heat flux in the convection zone by employing the MLT. However, his approach is to consider the inward energy access to be the energy access of an outward-moving convective element. He avoided the direct expansion regarding the mixing length so there is no limitation for the mixing length as it remains uncertain in his derivation. But the method is generated from the same idea.

### 3. TOKAMAK TRANSPORT

#### A. Dimensionless number

In this section, we present some simple applications of mixing length ideas to tokamak transport. Let’s represent the tokamak by a quasi-2D model like shown in FIG. 3.

Here we consider a Rossby number  $Ro \sim v_{\perp} \Omega \ll 1$ . Therefore, the quasi-2D cell has a coarse grid in the parallel direction ( $k_{\perp} \gg k_{\parallel}$ ). We also consider  $\omega < \Omega$ , so we have  $E \times B$  advection

$$\tilde{\mathbf{v}}_{\perp} = \frac{c}{B} \mathbf{E} \times \hat{\mathbf{z}} \quad (3.1)$$

For the perturbation located at the resonant surface, the pitch of the magnetic field line matches with the pitch of the perturbation. For a periodic magnetic field perturbation  $\tilde{B} \sim e^{i(m\theta - n\phi)}$ , the pitch of the magnetic field which can be represented by the safety factor  $q$  has

$$q = r B_T / R B_{\theta} = m/n \quad (3.2)$$

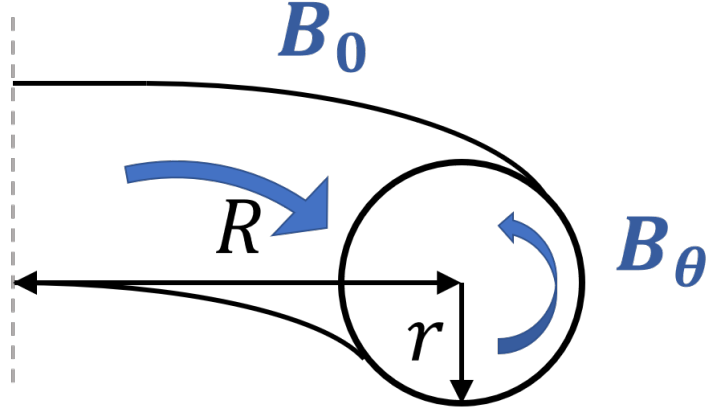


FIG. 3. A schematic of the steady-state velocity profile of pipe flow with a no-slip boundary condition. The red curve denotes the  $x$ -component velocity distribution with  $y$ .

At the resonant surface ( $\mathbf{k} \cdot \mathbf{B} = 0$ ), we have  $k_{\parallel} = 0$ . Since  $k_{\parallel}$  is a function of radius  $r$ , inside the resonant surface we have

$$\mathbf{k} \cdot \mathbf{B}/|\mathbf{B}| = k_{\parallel}(r) \quad (3.3)$$

We are particularly interested in the perturbations on the resonant surface. For  $k_{\parallel} = 0$ , there won't be any contributions from the bending energy of the magnetic field to the energy principle. Also, at  $k_{\parallel} = 0$ , there would be no Landau damping due to the vanishing of  $k_{\parallel}v_{\parallel}$  term. Therefore, perturbation takes place at the resonant surface. In other words, the turbulence are 'pinned' on the resonant surface of the plasma.

To study the turbulence transport, let us first look at the dimensionless numbers  $R_e = vL/\nu$ . The first thing comes to mind might be the Reynolds number. However, the Reynolds number is irrelevant in this story because the dissipation is not generally due to viscosity. The number which is relevant is the Kubo number  $Ku$ . The Kubo number is the ratio of the scattering length over the correlation length

$$Ku \sim \delta x/\Delta \sim \int \tilde{v} dt/\Delta \sim \tilde{v}\tau_c/\Delta, \quad (3.4)$$

where  $\tilde{v}$  is the velocity perturbation,  $\tau_c$  is the correlation time and  $\Delta$  is the correlation length. A small Kubo number ( $Ku < 1$ ) means there many perturbation with in one correlation length. In this case the transport can be considered as diffusive. For a large Kubo number ( $Ku > 1$ ), this means the scattering length is larger than the correlation length. Therefore, the system can be considered as strong scattering and highly nonlinear.



(Akin to the Kubo number in fluid turbulence transport, we can also get a magnetic Kubo number to study the field line transport in magnetic turbulence. The magnetic Kubo number can be defined as

$$Ku \sim \frac{\delta B l_{\parallel}}{B_0 l_{\perp}}, \quad (3.5)$$

where  $\delta B$  is the fluctuation of the magnetic field and  $B_0$  is the average field.  $l_{\perp}$  and  $l_{\parallel}$  respectively denote the correlation length in the perpendicular and parallel direction.)

In reality the tokamak is generally in a cross-over regime, where the Kubo number is at  $Ku \sim 1$  and we have a saturated turbulence. Generally, we can estimate the perturbation strength by

$$\tilde{v} \sim \Delta/\tau_c \quad (3.6)$$

Most of the turbulence we encountered in magnetic confinement is not strong turbulence ( $Ku \leq 1$ ). It is more akin to the wave turbulence rather than the fluid turbulence with high Reynolds number. Generally, the wave turbulence has a form with a quadratic nonlinear term, like

$$\partial_t a \sim Caa + \dots, \quad (3.7)$$

$$\partial_t \varepsilon \sim \partial_t |a|^2 \sim C\langle aaa \rangle + \dots, \quad (3.8)$$

where  $a$  denotes the wave amplitude and  $C$  is a coupling coefficient. From Eq. 3.8, we know that the energy transfer of the turbulence is resulted by three modes interaction (or ‘triad interaction’). Therefore, the key physics is important to study the triad coherence time.

A reasonable way to study the triad coherence time would be to relate the triad coherence time  $\tau_c$  to the rate of energy evolution  $\frac{1}{\varepsilon} \frac{\partial \varepsilon}{\partial t}$ , which is the inverse of the characteristic time scale of energy evolution  $\tau_{\varepsilon}$ . For the wave turbulence, the triad coherence time is usually small

$$\frac{1}{\varepsilon} \frac{\partial \varepsilon}{\partial t} \tau_c < 1 \quad (3.9)$$

This means the turbulence is weak and we have many kicks within the time scale of energy evolution.

Although the turbulence is weak, the dynamic range of the turbulence is quite large. Usually we can expect a large dynamic range in strong turbulence. In Kolmogorov 1941 (K41) Theory, the dynamic range is the ratio of excitation length scale  $l_0$  to the dissipation

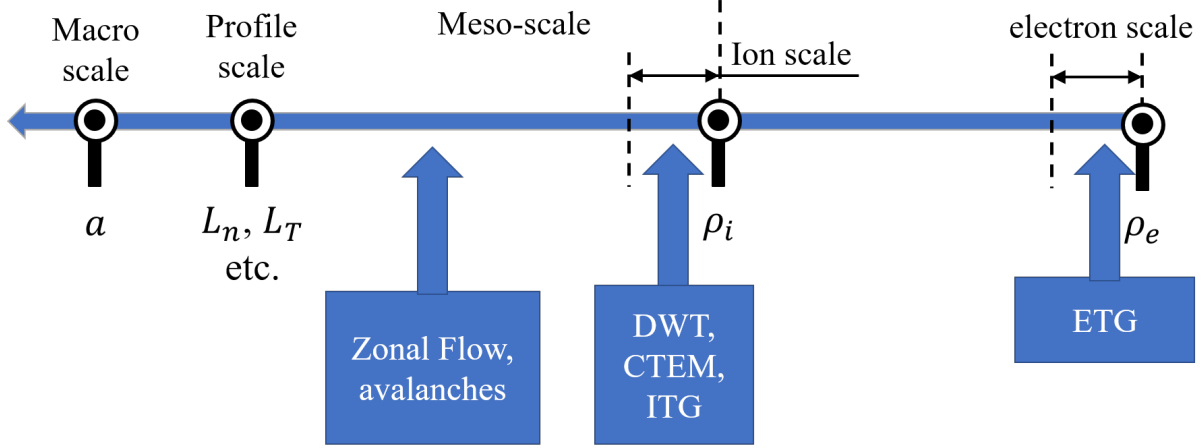


FIG. 4. The ‘zoo’ of length scale in tokamak (ordered in increasing length from right to left). Here,  $a$  denotes the system size.  $L_n, L_T$  is respectively the length scale of density and temperature gradient. DWT is the drift wave turbulence. CTEM is the collisionless trapped electron mode. ITG is ion temperature gradient. ETG is the electron temperature gradient.

length scale  $l_d$ . The excitation length scale comes from the energy flux

$$\varepsilon \sim v^3/l_0, \quad (3.10)$$

The dissipation scale is related to Kolmogorov dissipation scale, which is

$$l_d \sim \left(\frac{\nu^3}{\varepsilon}\right)^{1/4}. \quad (3.11)$$

Therefore, the dynamic range has

$$\frac{l_0}{l_d} \sim \left(\frac{\nu l_0}{\nu}\right)^{3/4} \sim Re^{3/4} \quad (3.12)$$

Therefore, for strong turbulence with  $Re \gg 1$ , we would get a larger dynamic range of the turbulence. While in plasma turbulence, you can have a weak turbulence and a large dynamic range. That is the difference.

## B. Dynamic range of DWT

From FIG. 4, we can see that there is a large range of length scale in tokamak. The ratio of the largest scale to the smallest scale is pretty big. Unlike the pipe flow we talked about in Section. 1, there are two dynamic scales for the drift wave turbulence. The first scale

is the gyro-radius of the ions  $\rho_i$ . It sets the minimum of the non-dissipative length scale. (There is no corresponding scale for  $\rho_i$  in the case for the pipe flow. )The other one is the macroscopic scale, like the system size  $a$  or or the length scale of the temperature profile  $L_T$ . (In the case for the pipe flow, this corresponds to the distance to the wall  $y$ .) Here, we set a key smallness parameter  $\rho_*$  as

$$\rho_* = \rho_i/L_T \ll 1 \quad (3.13)$$

The smallness parameter  $\rho_*$  is of great interest in terms of size scaling in tokamak. The question we want to answer here is: what is the best optimized scale for magnetic confinement? Is ‘bigger always better’?

To further understand the transport inside tokamak, we need to look at the mixing length we talked about in Section 2. The mixing length will be a length scale between  $\rho_i$  to  $\rho_i/\rho_*$ , so we can set

$$l_{mix} \sim L_T \rho_*^\alpha \quad (3.14)$$

where  $\alpha$  is a parameter ranging from 0 to 1.

Also, in analogous to the case in the pipe flow that the diffusivity can be expressed as  $u_* y$ , the diffusivity for the drift wave turbulence can be expressed as

$$D \sim \tilde{v} l_{mix}, \quad (3.15)$$

where the typical velocity  $\tilde{v}$  is the diamagnetic velocity  $v_d \sim \rho_* C_s$ .

We can rewrite the diffusivity as

$$\begin{aligned} D &\sim \rho_* C_s L_T \rho_*^\alpha \\ &\sim \rho_i C_s \rho_*^\alpha \end{aligned} \quad (3.16)$$

Noticed that  $\rho_i C_s$  has a dimension of diffusivity, we find that it is related to Bohm diffusion

$$\boxed{D \sim D_B \rho_*^\alpha} \quad (3.17)$$

Here,  $D_B \sim T/B$  is the Bohm diffusivity. If  $\alpha = 0$ , then the diffusion is simply Bohm diffusion. In this case, ‘bigger is not better’. For  $\alpha = 1$ , the diffusion becomes Gyro-Bohm Diffusion

$$D \sim D_{GB} \sim D_B \rho_* \sim \rho_i^2 C_s / L_T \quad (3.18)$$

Because the energy confinement time  $\tau_E \sim L_T^2/D$ , so

$$\tau_E \sim L_T^3 \sim a^3. \quad (3.19)$$

In this case, indeed, ‘bigger is better’.

Again, the reality is usually somewhere in between. In reality, we usually have  $0 < \alpha < 1$ , which we called the Broken Gyro-Bohm Diffusion. Typically, an ad hoc approach to evaluate the mixing length would be the geometric mean of the gyro radius times the profile length scale,

$$l_{mix} \sim (\rho_i L_T)^{1/2}. \quad (3.20)$$

The smallness parameter  $\rho_*$  is complicated by the multi-zone structure of the confinement in tokamak. For example, in H-mode, the confinement physics in the core and pedestal is different. It is still an ongoing study about how we can come up with a global scaling.

An example for the Bohm Diffusion model is to look at the analogous question in the Rayleigh Benard Convection. The key study the dimensionless parameters in this heat transfer is to compare the Nusselt Number ( $Nu$ ) with the Rayleigh number

$$Nu \sim \frac{\langle \tilde{v}\tilde{T} \rangle}{\chi \Delta T / h} \quad (3.21)$$

$$Re \sim \frac{h^3 g \alpha \Delta T}{\chi \nu} \quad (3.22)$$

where  $\chi$  is the thermal diffusivity,  $\alpha$  is the expansion coefficient. Nusselt number denotes the ratio of the convective heat flux and the conductive heat flux. The Rayleigh number describes the strength of the drive.

The emperical observation of Rayleigh Benard Convection tells us that the temperature gradient is mostly located at the boundary layer, which is akin to the boundary confinement in H-mode. The temperature density in the core is flat, so the size doesn’t really matter (‘bigger does not mean better’). In other words, the heat flux  $\langle \tilde{v}\tilde{T} \rangle$  should be independent of the box size. Therefore,

$$Nu \sim \langle \tilde{v}\tilde{T} \rangle h / \chi \Delta T \quad (3.23)$$

Notice that  $Ra \sim h^3$ , so

$$\boxed{Nu \sim (Ra)^{1/3}} \quad (3.24)$$

This scaling is well supported by the simulation and experimental result.

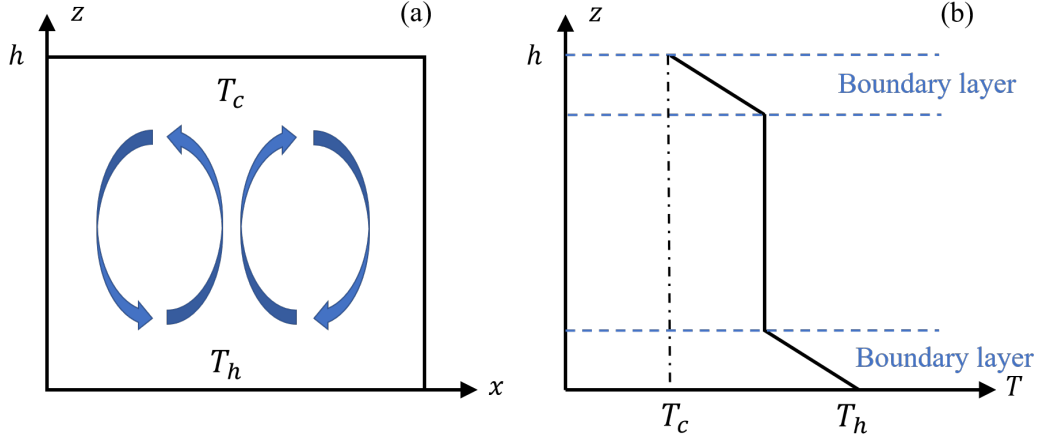


FIG. 5. (a) A schematic figure of Rayleigh-Bénard Convection inside the box. (b) A schematic figure of the temperature evolution in the horizontal direction.

### C. Theoretical view of the diffusion

To revisit our discussion on Bohm and Gyro Bohm diffusion in a theoretical view, we can calculate the diffusion coefficient in the Kubo formalism

$$D_{\perp} \sim \int_0^{\infty} \langle \tilde{v}(0) \tilde{v}(-\tau) \rangle d\tau \quad (3.25)$$

Here, we consider a quasi-2D system and we are considering ions. So the velocity will be the sum of  $E \times B$  drift

$$v_{\perp} \sim \frac{c}{B_0} \sum_k E_{\perp,k} \exp(i\mathbf{k} \cdot \mathbf{r}) \quad (3.26)$$

$$D_{\perp} \sim \int_0^{\infty} d\tau \sum_k |\tilde{v}_k|^2 \langle \exp(-i\mathbf{k} \cdot \mathbf{r}(0)) \cdot \exp(-i\mathbf{k} \cdot \mathbf{r}(-\tau)) \rangle \quad (3.27)$$

where  $\tilde{\mathbf{v}}_k = \frac{c}{B} \tilde{\mathbf{E}}_{\perp} \times \hat{\mathbf{z}}$ . For a statistical model, we can express  $r(-\tau)$  as

$$\mathbf{r}(-\tau) = \mathbf{r}(0) + \delta\mathbf{r}(-\tau) \quad (3.28)$$

where  $\delta r(-\tau)$  is a kick due to scattering which is stochastic. Therefore, the diffusion coefficient has

$$D_{\perp} \sim \int_0^{\infty} d\tau \sum_k |\tilde{v}_k|^2 \langle \exp(i\mathbf{k} \cdot \delta\mathbf{r}(-\tau)) \rangle \quad (3.29)$$

Because  $\delta\mathbf{r}(-\tau)$  is a small value, we can Taylor expand the equation

$$\begin{aligned}
D_{\perp} &\sim \int_0^{\infty} d\tau \sum_k |\tilde{v}_k|^2 \langle 1 + i\mathbf{k} \cdot \delta\mathbf{r}(-\tau) - \frac{(\mathbf{k} \cdot \delta\mathbf{r}(-\tau))^2}{2} + \dots \rangle \\
&\sim \int_0^{\infty} d\tau \sum_k |\tilde{v}_k|^2 \langle 1 - \frac{(\mathbf{k} \cdot \delta\mathbf{r}(-\tau))^2}{2} + O(\delta\mathbf{r}^3) \rangle \\
&\sim \int_0^{\infty} d\tau \sum_k |\tilde{v}_k|^2 (1 - k_{\perp}^2 D_{\perp} \tau) \\
&\sim \int_0^{\infty} d\tau \sum_k |\tilde{v}_k|^2 (1 - \exp(-k_{\perp}^2 D_{\perp} \tau)) \\
&= \sum_k |\tilde{v}_k|^2 / k_{\perp}^2 D_{\perp}
\end{aligned} \tag{3.30}$$

So we can see that the diffusion coefficient  $D_{\perp}$  controls the correlation time  $\tau_c$ . Also, the strong scaling of  $k_{\perp}$  which comes from the fact that the particle number is conserved ( $\partial_t \int n \cdot d\mathbf{x} = 0$ ). It ensures a long correlation time  $\tau_c$  at large scale.

The diffusion can be expressed as

$$D_{\perp} \sim \left( \sum_k |\tilde{v}_k|^2 / k_{\perp}^2 \right)^{1/2} \tag{3.31}$$

We can go further to say that it has a symmetric spectrum in 2D and rewrite the expression as

$$D_{\perp} \sim \left( \int_0^{\infty} |\tilde{v}_k|^2 / dk_{\perp} \right)^{1/2} \tag{3.32}$$

This is telling us that the spectrum structure, especially the infrared scaling, is important in diffusion.

Recall from Eq. (3.15) and compare it to Eq. (3.32), we can see that

$$l_{mix} \sim k_{\perp}^{-1} \tag{3.33}$$

$$v_{rk} \sim \frac{c}{B} i k_{\theta} \hat{\phi}_k \tag{3.34}$$

Therefore, the mixing length is determined by the structure of the spectrum.

To estimate the potential, we can rewrite Eq. (3.34) as,

$$v_{rk} \sim k_{\theta} \rho_i C_s |e| \hat{\phi}_k / T \tag{3.35}$$

Recall that in drift wave turbulence, the phase velocity is between the thermal velocity of electrons and ions ( $v_{thi} < \omega / k_{\parallel} < v_{the}$ ). With the phase velocity slower than the electrons,

the density satisfies the Boltzmann relation  $\tilde{n}/n \sim |e|\hat{\phi}/T$ . We can rewrite Eq. (3.34) and Eq. (3.32) as,

$$\tilde{v} \sim k_\theta \rho_i C_s \frac{\tilde{n}}{n} \quad (3.36)$$

$$D \sim D_B k_\theta \frac{\tilde{n}}{n} l_{mix} \quad (3.37)$$

This is the general basic scaling for the diffusion in drift wave turbulence.

A good estimation on  $\tilde{n}/n$  is conducted by Kodemtsev in 1965. The idea is to write down the continuity equation and evaluate when the nonlinear term saturates with the linear term

$$\partial_t \tilde{n} + \tilde{\mathbf{v}} \cdot \nabla \tilde{n} = -\tilde{\mathbf{v}} \cdot \nabla \langle n \rangle \quad (3.38)$$

$$\tilde{v} k_r \tilde{n} = -\tilde{v} \frac{\partial \langle n \rangle}{\partial r} \sim -\tilde{v} n / L_n \quad (3.39)$$

And we can get the estimate of  $\tilde{n}/n$

$$\tilde{n}/n = \frac{1}{k_r L_n} \quad (3.40)$$

Substitute back to Eq. (3.37), we get

$$D = D_B \frac{k_\theta}{k_r L_n} l_{mix} \quad (3.41)$$

If the system is isotropic than  $k_\theta/k_r$  vanish,

$$D = D_B \frac{l_{mix}}{L_T} \sim D_B \rho_*^\alpha \quad (3.42)$$

which comes back to our argument in Eq. (3.17).

#### D. Effect of shear flow

If we are looking at the case with a shear flow, how would things change? We can go back to our derivation of 3.28. In the case of  $E \times B$  shear flow, for  $\delta r$  there are two contributors, the stochastic kick and the shear flow

$$\delta r = -v_y \tau + \delta r_s(-\tau) \quad (3.43)$$

where  $\delta r_s$  means the stochastic kick. We can express things in terms of shear

$$\delta r = -v'_y \int_0^\tau x \tau + \delta r_s(-\tau) \quad (3.44)$$

Here  $v'_y$  is the velocity gradient in shear flow ( $\mathbf{v}_y = (v_y(0) + xv'_y)\hat{\mathbf{y}}$ ). Noticed that the particle radial position  $x$  is scattered , so

$$\delta r = -v'_y \int_0^\tau \delta x(-\tau') d\tau' + \delta r_s(-\tau) \quad (3.45)$$

Going back to Eq. (3.27), we get

$$D_\perp \sim \int_0^\infty d\tau \sum_k |\tilde{v}_k|^2 \langle \exp(ik_y v'_y \int_0^\tau \delta x(-\tau') d\tau') \cdot \exp(i\mathbf{k} \cdot \delta \mathbf{r}(-\tau)) \rangle \quad (3.46)$$

Therefore, the shearing actually couples the streaming and scattering process. This leads to an enhanced decorrelation.

$$D_\perp \sim \int_0^\infty d\tau \sum_k |\tilde{v}_k|^2 \langle \exp(ik_y^3 v_y'^2 D_r \tau^3 / 3) \cdot \exp(i\mathbf{k} \cdot \delta \mathbf{r}(-\tau)) \rangle \quad (3.47)$$

Therefore, the correlation time now has

$$\tau_c = (K_y^2 v'_y D_r / 3)^{-1/3} \quad (3.48)$$

A important point worth noticing is that now correlation time depends on  $k_y$  rather than  $k_r$  like we previously talked about ( $1/\tau_\perp \sim k_r^2 D_r$ ). This means that the shear has broken the relation of mixing length and scattering,

Another point worth mentioning is the two time history in the diffusion

$$D_\perp \sim \int_0^\infty d\tau \sum_k |\tilde{v}_k|^2 \langle \exp(-(\tau/\tau_c)^3 - \tau/\tau_\perp) \rangle \quad (3.49)$$

The second term in the exponential is like what we talked about in Section. 3.C. However, if the first term is dominant, which means  $(K_y^2 v'_y D_r)^{1/3} > k_r^2 D_r$ , then

$$k_y v'_y \Delta r > k_r^2 D \quad (3.50)$$

where  $\Delta r$  is the radial coherent scale ( $1/k_r^2 \sim \Delta r$ ) Then the diffusion can be written as

$$\begin{aligned} D &\sim \int_0^\infty d\tau \sum_k |\tilde{v}_k|^2 \langle \exp(-(\tau/\tau_c)^3) \rangle \\ &\sim \sum_k |\tilde{v}_k|^2 \tau_c \\ &\sim \sum_k |\tilde{v}_k|^2 \tau_\perp \frac{\tau_c}{\tau_\perp} \end{aligned} \quad (3.51)$$



Because  $\tau_c/\tau_\perp < 1$ , therefore the diffusion went down. Therefore, sheath is good for confinement.

We can also get some further estimate with Eq. (3.51)

$$D \sim \sum_k |\tilde{v}_k|^2 (K_y^2 v_y'^2 D)^{-1/3} \quad (3.52)$$

$$D^{4/3} \sim \sum_k |\tilde{v}_k|^2 (K_y^2 v_y'^2)^{-1/3} \quad (3.53)$$

We can see that the diffusion is still sensitive to low  $k_y$  like we previously discussed.

The bottom line here is shear is good for confinement. It reduces diffusion and drive us away from Bohm Diffusion.